Legends to supplementary figures

Figure S1. 786-O and A498 cells show different sensitivities to ERLO. Quantification of immuno-blots (three independent experiments), the representative images was shown on Fig. 1D. 786-O or A498 cells were treated with increasing concentrations of ERLO and were tested for the presence of total (EGFR/HSP90), the active form of the EGF receptor (pEGFR/EGFR), the active form of AKT (pAKT/HSP90) and the active form of ERK (pERK/ERK). The statistical significance for the different ERLO concentrations for a specific cell line is shown by * (* $p < 0.05$; ** $p < 0.01$). The statistical significance for the comparison of the two cell lines is shown by # (# $p < 0.05$; ## $p < 0.01$).

Figure S2. BVZ/IFN/ERLO on the vascular/lymphatic networks. The tumor vascular/lymphatic networks in each experimental group (control, B+I, E, B+I+E) were evaluated by CD31 immuno-staining and coverage of the vessels using an anti-⟨SMA antibody as presented on Fig. 2. Vascular/lymphatic density (vessels/mm^2) and the number of vessels covered with ⟨SMA labelled cells were determined using the Image J program. Quantification (means ± SD) resulted from analysis of four independent tumors and considered at least ten fields for each tumour. Statistically significant differences are indicated: * $p < 0.05$; ** $p < 0.01$; *** $p < 0.001$.

Figure S3. Differential inhibition of proliferation-mediating signaling pathways by ERLO in cells derived from experimental tumors. **(A)** Representative 786-O cells from the four experimental groups were tested for the presence of the total and active form of the EGF receptor (EGFR/pEGFR, see Fig. 3) and active forms of ERK (pERK) and AKT (pAKT). HSP90 is shown as a loading control. Quantification of the relative level of EGFR (EGFR/HSP90), pEGFR (pEGFR/EGFR), pERK (pERK/HSP90) and pAKT (pAKT/HSP90)

is shown (Fig. 3). The reference values (100%) correspond to the levels of the different parameters in cells of tumors derived from untreated mice in the absence of ERLO. **(B)** Equivalent experiments as described in **(A)** for the A498 model.

Figure S4. Parental 786-O cells proliferated faster than A498 parental cells. The proliferative capacity of parental 786-O and A498 cells was tested using the MTT assay. The results are presented as the mean percent increase ± s.d. Statistical differences are indicated; ** $p < 0.01$; *** $p < 0.001$.

Figure S5. RCC4, 786-O and A498 cells expressed different EGFR and EGFR-AS1 levels. **(A)** EGFR mRNA levels were evaluated by qPCR in RCC4, 786-O and A498 cells; **, $p<0.01$. **(B)** Representative immuno-blots showing the EGFR protein level in the different RCC cell lines after treatment in the absence or presence of increasing concentrations of ERLO. HSP90 is shown as a loading control. **(C)** Quantification in three independent experiments for EGFR levels in the different cell lines and in response to ERLO. ** $p < 0.01$; *** $p < 0.001$. **(D)** EGFR-AS1 mRNA levels were evaluated by qPCR in RCC4, 786-O and A498 cells; ***, $p<0.001$.

Figure S6. EGFR levels are correlated to RCC aggressiveness depending on the metastatic status. **(A)** Graph showing relative levels of EGFR transcript in RCC tumors of different stages versus normal tissue measured by RNA-seq data available from TCGA. p values are indicated. **(B)** The Kaplan–Meier analysis of overall survival (OS) of patients with M0 RCC from the TCGA data base. OS was calculated from patient subgroups with an optimized cut-off for EGFR levels. **(C)** The Kaplan–Meier analysis of overall survival of patients with M1 RCC from the TCGA data base. Overall survival was calculated from patient subgroups with an optimized

cut-off for EGFR levels. **(D)** The Kaplan–Meier analysis of disease-free survival (DFS) of patients with M0 RCC from the TCGA data base. DFS was calculated from patient subgroups with an optimized cut-off for EGFR levels. **(E)** The Kaplan–Meier analysis of progression-free survival (PFS) of patients with M1 RCC from the TCGA data base. PFS was calculated from patient subgroups with an optimized cut-off for EGFR levels.

Figure S7. EGFR-AS1 levels are correlated to RCC aggressiveness depending on the metastatic status. **(A)** Graph showing relative levels of EGFR-AS1 (1) transcript in RCC tumors of different stages versus normal tissue measured by RNA-seq data available from TCGA. p values are indicated. **(B)** The Kaplan–Meier analysis of overall survival (OS) of patients with M0 RCC from the TCGA data base. OS was calculated from patient subgroups with an optimized cut-off for EGFR-AS1 levels. **(C)** The Kaplan–Meier analysis of OS of patients with M1 RCC from the TCGA data base. OS was calculated from patient subgroups with an optimized cut-off for EGFR-AS1 levels. **(D)** The Kaplan–Meier analysis of disease-free survival (DFS) of patients with M0 RCC from the TCGA data base. DFS was calculated from patient subgroups with an optimized cut-off for EGFR-AS1 levels. **(E)** The Kaplan–Meier analysis of progression-free survival (PFS) of patients with M1 RCC from the TCGA data base. PFS was calculated from patient subgroups with an optimized cut-off for EGFR-AS1 levels.

Reference

1. Tan DSW, Chong FT, Leong HS, Toh SY, Lau DP, Kwang XL*, et al.* Long noncoding RNA EGFR-AS1 mediates epidermal growth factor receptor addiction and modulates treatment response in squamous cell carcinoma. Nat Med **2017**;23:1167-75

	FORWARD	REVERSE
Housekeeping genes		
36B4	CAGATTGGCTACCCAACTGTT	GGCCAGGACTCGTTTGTACC
m-36B4	AGATTCGGGATATGCTGTTGGC	TCGGGTCCTAGACCAGTGTTC
GAPDH	TGC ACC ACC AAC TGC TTA GC	GGC ATG GAC TGT GGTCAT GAG
Pro/Anti-angiogenesis genes		
m-CD31	ACGCTGGTGCTCTATGCAAG	TCAGTTGCTGCCCATTCATCA
m-NG2	ACTAACCCATGCACTACATCAAG	ACTTTTCCAGACAGAGAGCCTT
m-αSMA	GTC CCA GAC ATC AGG GAG TAA	TCG GAT ACT TCA GCG TCA GGA
IL6	CCTGAACCTTCCAAAGATGGC	TTCACCAGGCAAGTCTCCTCA
CXCL5	AGCTGCGTTGCGTTTGTTTAC	TGGCGAACACTTGCAGATTAC
CXCL4	AGCCACGCTGAAGAATGGAA	CACACACGTAGGCAGCTAGT
CXCL10	GTGGCATTCAAGGAGTACCTC	TGATGGCCTTCGATTCTGGATT
Lymphangiogenesis genes		
mLYVE	CAG CACACTAGCCTGGTGTTA	CGCCCATGATTCTGCATGTAGA
m-VEGF-C	CTCTGTGGGACCACATGGTAA	TCCTCTCCCGCAGTAATCCA
Proliferation genes		
PTPRk	AATGCTCCTCCTCAGCTTCTTGGT	AGGACCATCGCCATTGATCGAGTT
EGFR	ATGCGACCCTCCGGGACGGC	CAAACGGTCACCCC TTTCTTTTCC
EGF	TGTCCACGCAATGTGTCTGAA	CATTATCGGGTGAGGAACAACC
m-EGFR	GCCATCTGGGCCAAAGATACC	GTCTTCGCATGAATAGGCCAAT
m-EGF	AGCATCTCTCGGATTGACCCA	CCTGTCCCGTTAAGGAAAACTCT
CSF1	TGGCGAGCAGGAGTATCAC	AGGTCTCCATCTGACTGTCAAT
m-CSF1	ATGAGCAGGAGTATTGCCAAGG	TCCATTCCCAATCATGTGGCTA
m-CSF1R	TGTCATCGAGCCTAGTGGC	CGGGAGATTCAGGGTCCAAG
Immune tolerance genes		
PDL1	TGGCATTTGCTGAACGCATTT	TGCAGCCAGGTCTAATTGTTTT
Macrophage M1 genes		
miNOS	TCACCTTCGAGGGCAGCCGA	TCCGTGGCAAAGCGAGCCAG
mIL6	ATCCAGTTGCCTTCTTGGGACTGA	TTGGATGGTCTTGGTCCTTAGCCA
Macrophage M2 genes		
mARG1	GATTATCGGAGCGCCTTTCT	CCACACTGACTCTTCCATTCTT
mCD206	CTGCAGATGGGTGGGTTATT	GGCATTGATGCTGCTGTTATG

Supplementary Table S1. List of oligo-nucleotides used in qPCR experiments

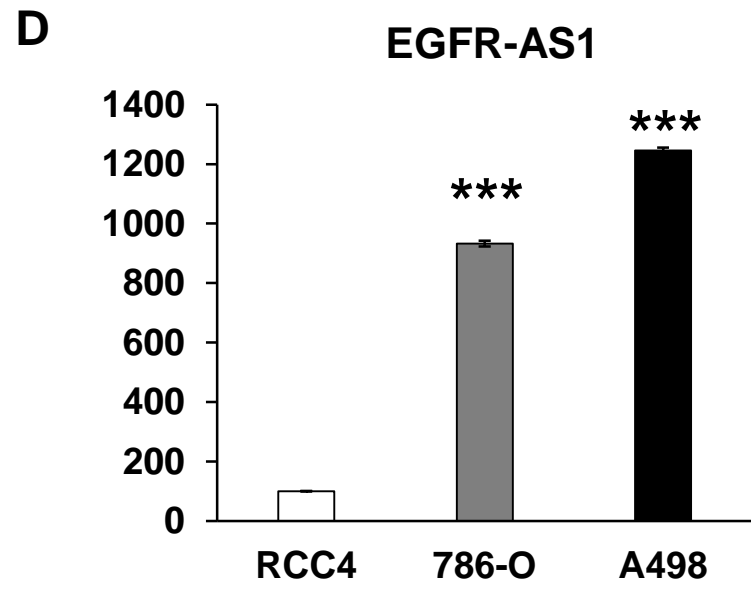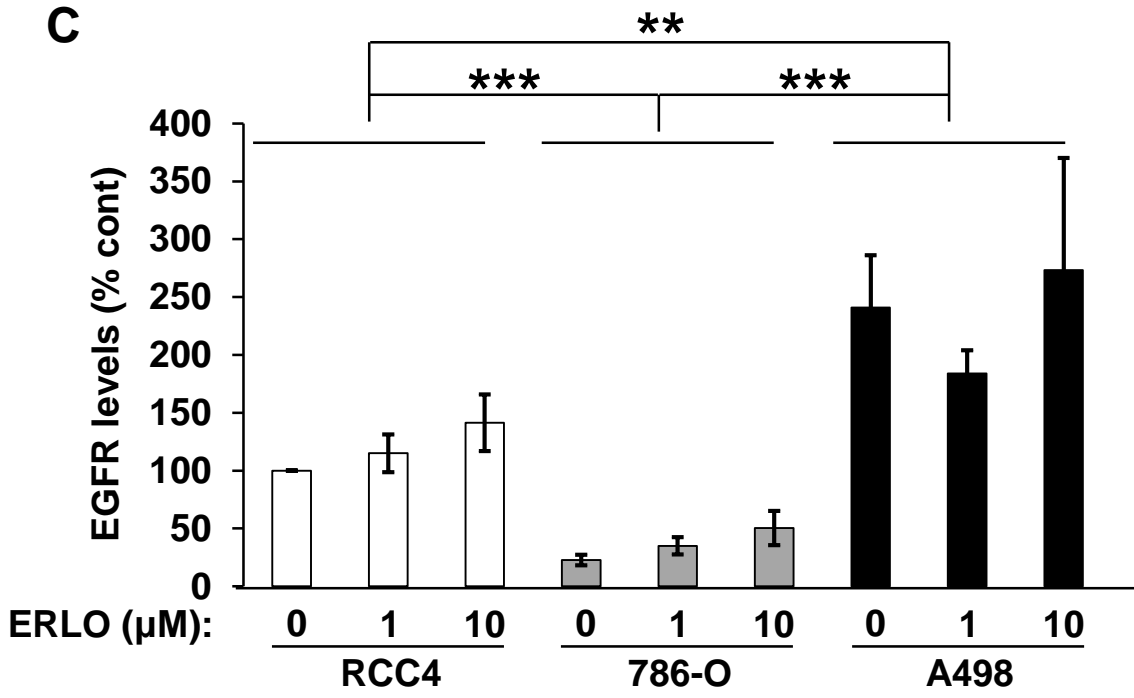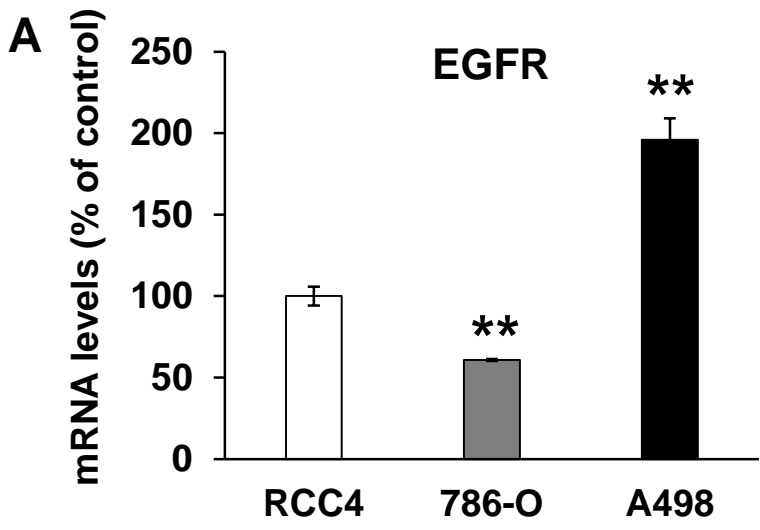|	ERLO (µM)	EGFR/HSP90	pEGFR/EGFR	pAKT/HSP90	pERK/ERK
	0	100	100	100	100
786-O	1	120	17 **	77 *	30 **
	10	140	1 **	53 *	30 **
	0	247 ##	1 #	14 #	279 ##
A498	1	184	5	23	198 *
	10	240	1	23	151 *

Supplementary Figure S1: Grépin *et al*

A

786-O	Control	B + I	E	B + I + E
CD31	10	6.6	6 (*)	4.75 (**)
CD31 + αSMA	0.75	3 (***)	2.25 (***)	1.25 (***)
LYVE1	1.2	4 (***)	2.3 (**)	1.6 (*)

B

| A498	Control	B + I	E	B + I + E
CD31	24	25	18.8	15.6 (**)
CD31 + αSMA	9.4	18.8 (***)	14.4 (***)	8.2 (*)
LYVE1	4.7	7.5 (**)	3.5 (***)	3.3 (***)

Supplementary Figure S2: Grépin *et al*

A

	C		B+I		E		B+I+E	
ERLO	−	+	−	+	−	+	−	+
EGFR								
pEGFR								
EGFR/HSP90	100	89	188	113	136	149	174	183
pEGFR/EGFR	100	86	100	47	100	42	100	47

pERK								
pAKT								
HSP90								
pERK/HSP90	100	141	100	48	100	70	100	68
pAKT/HSP90	100	120	100	55	100	23	100	87

B

	C		B+I		E		B+I+E	
ERLO	−	+	−	+	−	+	−	+
EGFR								
pEGFR								
EGFR/HSP90	100	95	79	81	85	100	75	76
pEGFR/EGFR	100	59	100	84	100	86	100	90

pERK								
pAKT								
HSP90								
pERK/HSP90	100	50	100	64	100	56	100	88
pAKT/HSP90	100	31	100	55	100	68	100	56
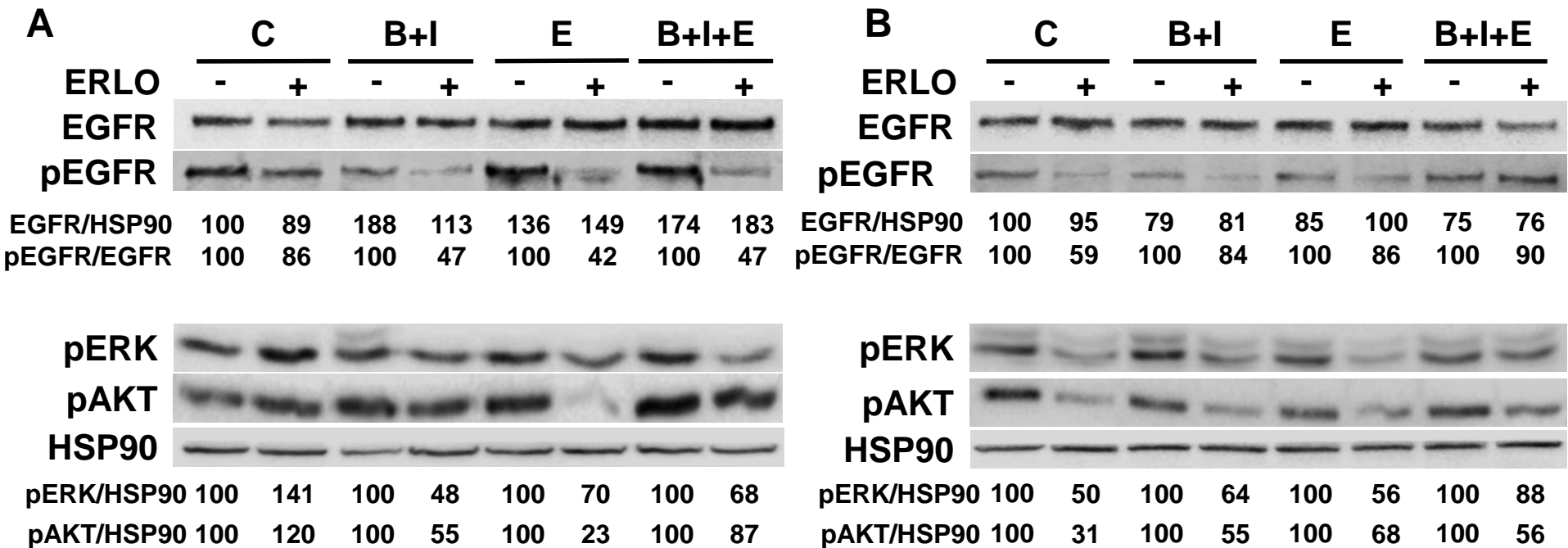
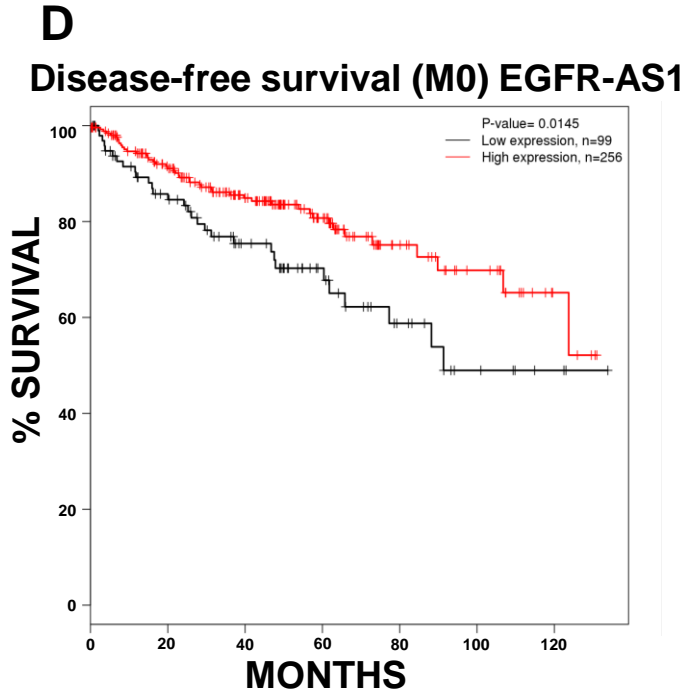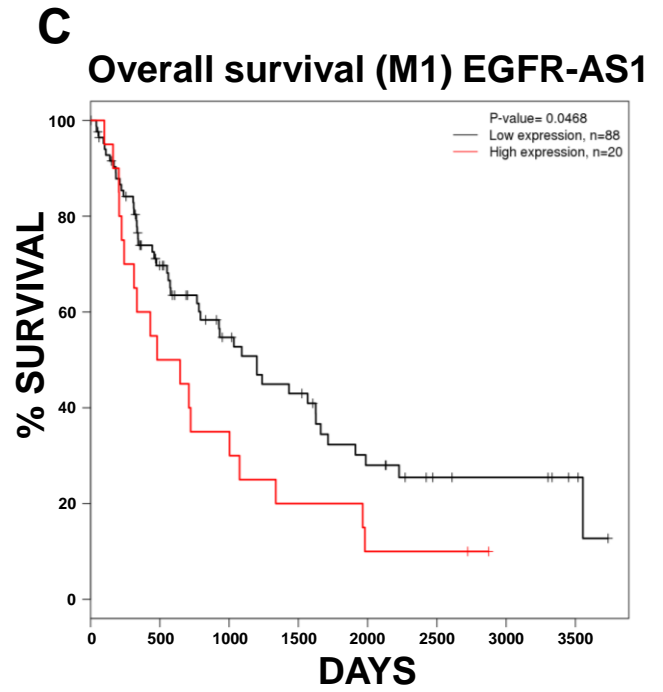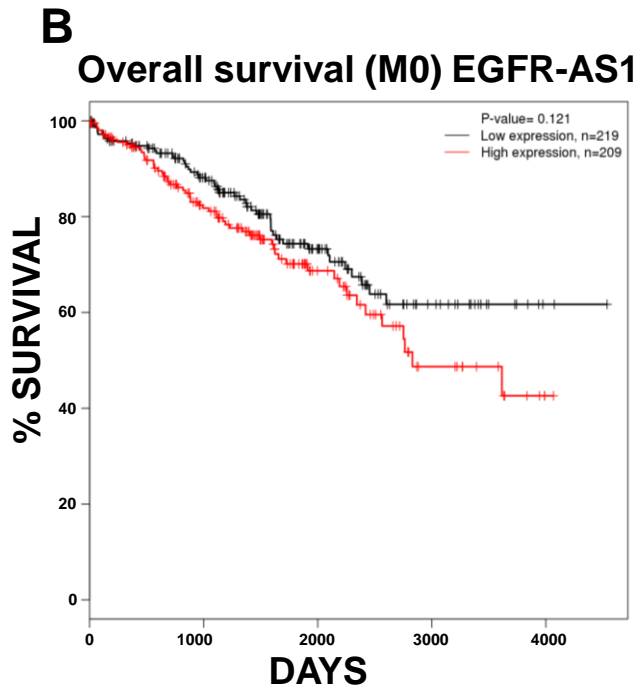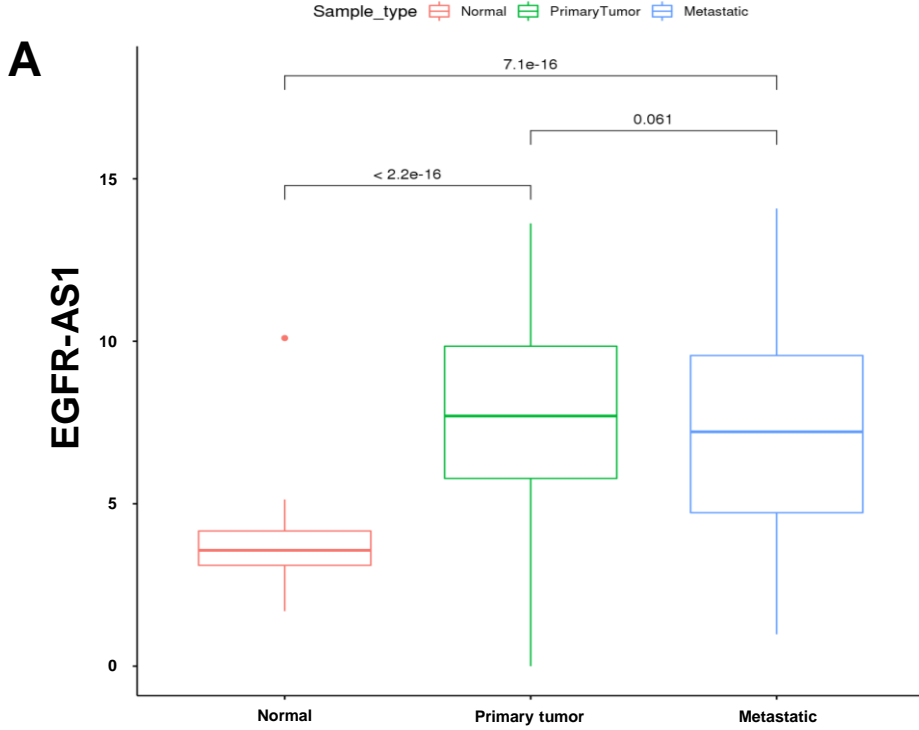**Supplementary Figure S3: Grépin *et al***
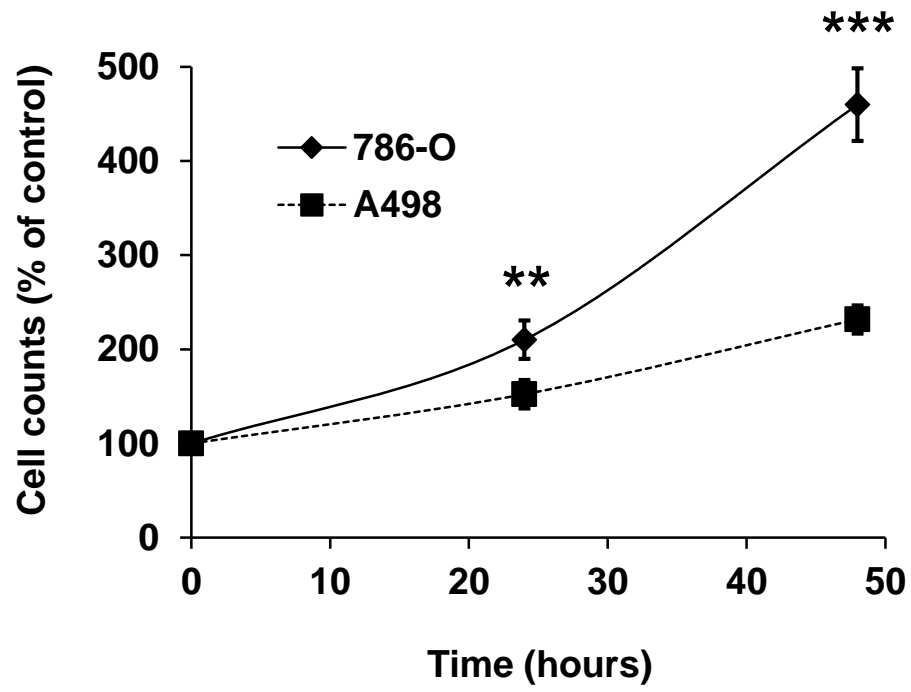
Supplementary Figure S4: Grépin *et al*

Supplementary Figure S5: Grépin *et al*
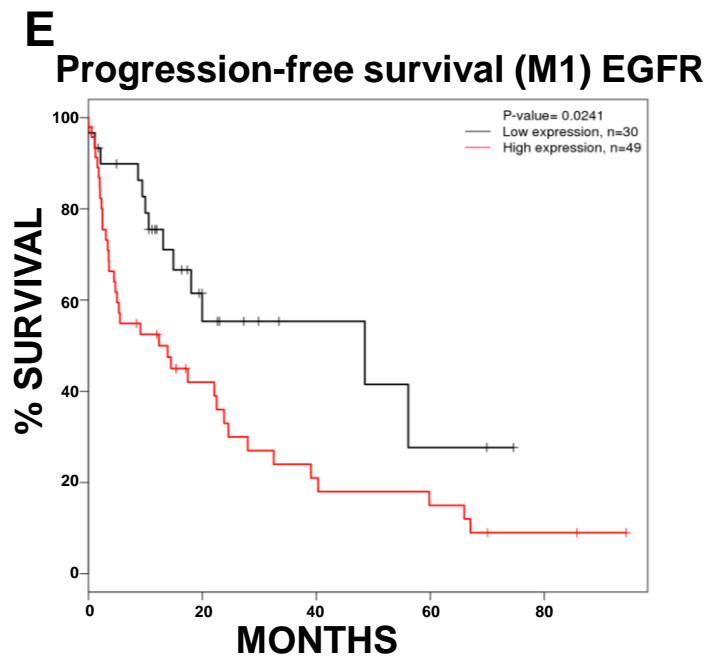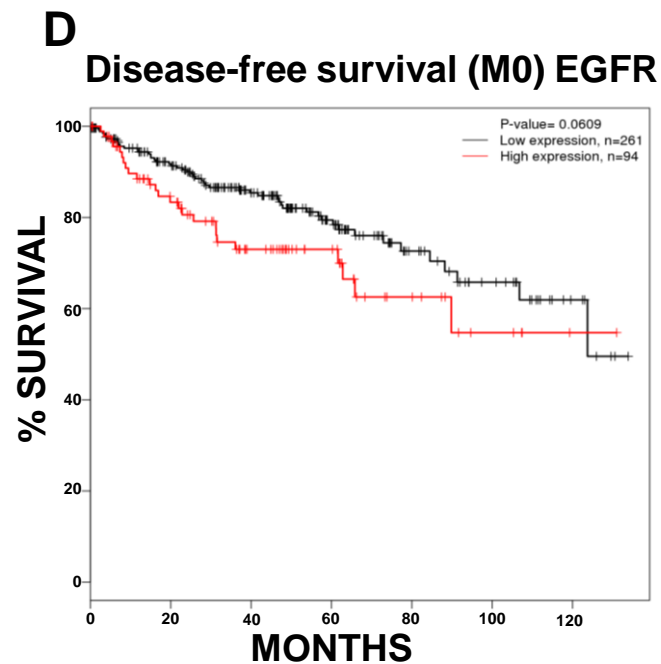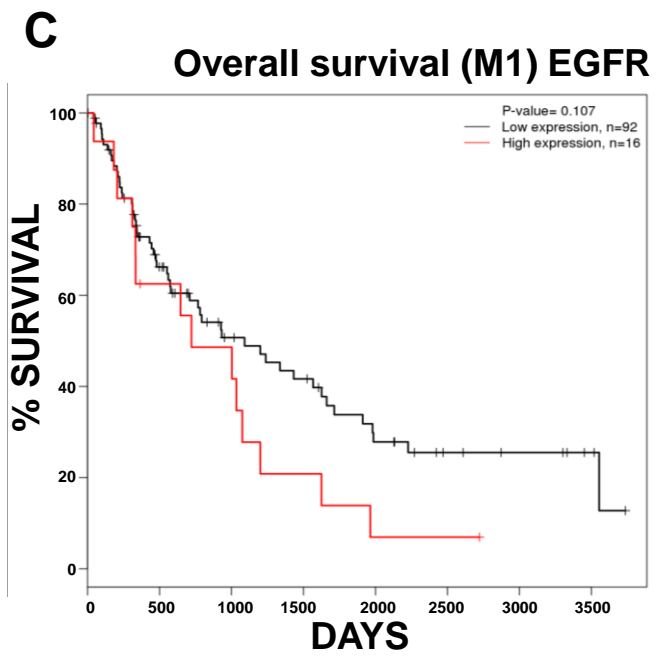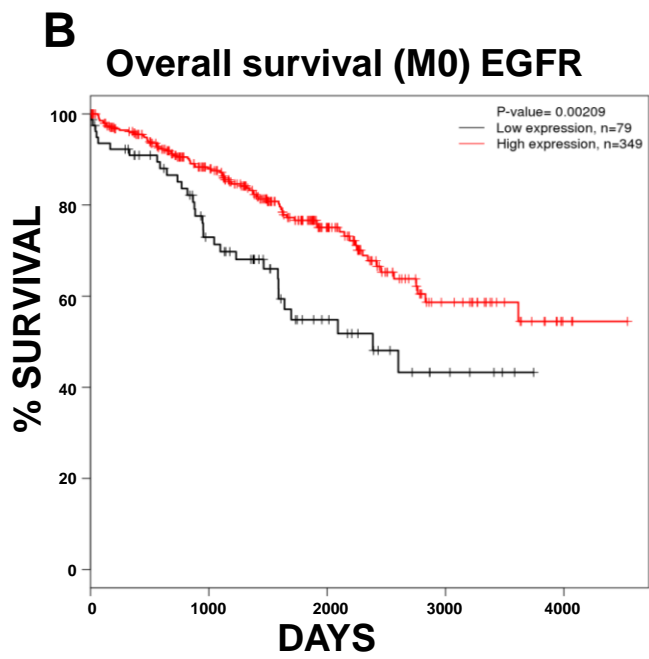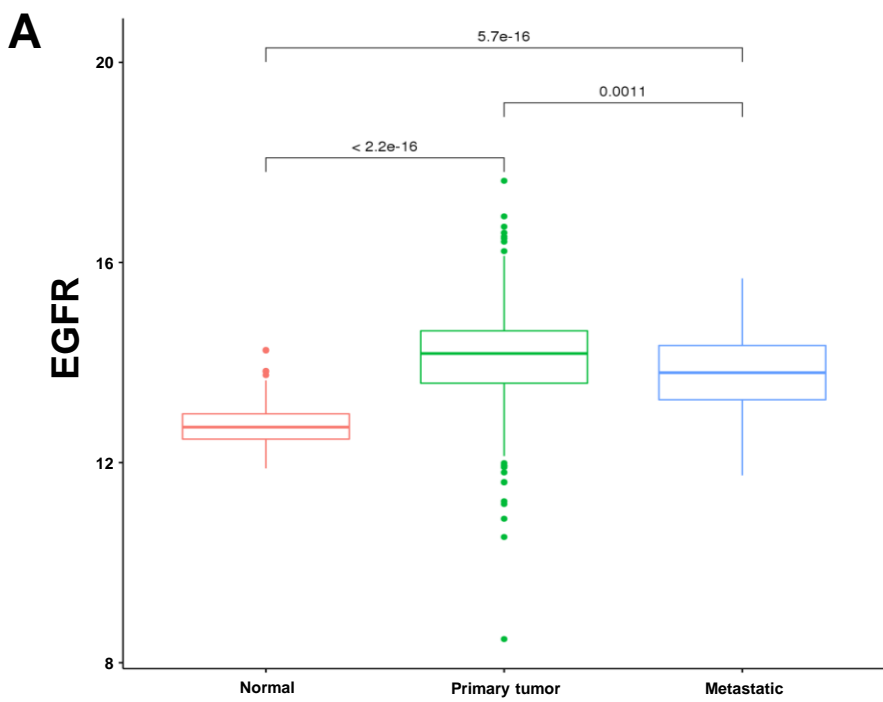
Supplementary Figure S6: Grépin *et al*
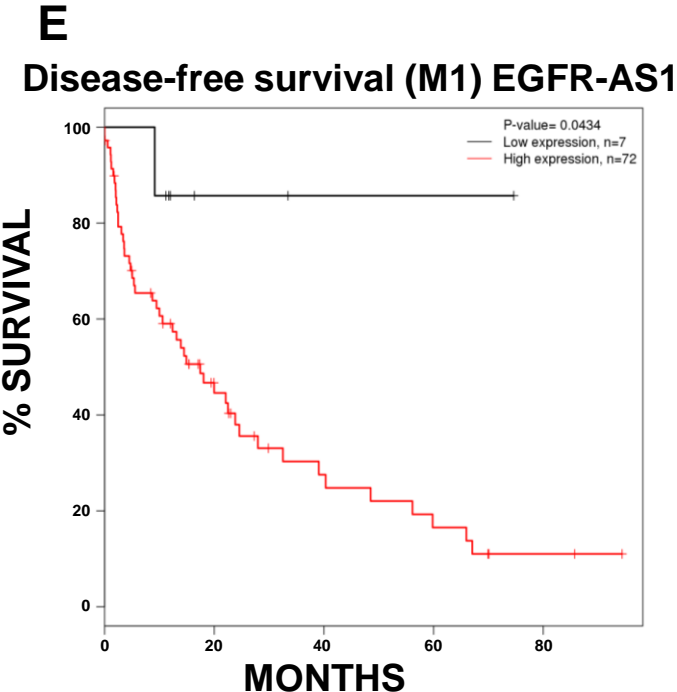
Supplementary Figure S7: Grépin *et al*